JPE 1-1-2

Performance Analysis of a Three-Phase Parallel Active Power Filter which Compensates PCC Voltage and the Unbalanced Loads

Woo-Cheol Lee*, Taeck-Kie Lee[1], and Dong-Seok Hyun

Hanyang University, Seoul, 133-791 Korea
[1]Hankyong National University, Ansung, Korea

ABSTRACT

The performance analysis of a three-phase parallel active power filter that compensates PCC voltage and the unbalanced loads is presented in this paper. The proposed scheme in this paper employs a PWM voltage-source inverter and has two operation modes. Firstly, it operates as a conventional active filter with reactive power compensation when PCC voltage is within the 15% voltage drop range. Secondly, it operates as a voltage compensator when PCC voltage is not within the 15% voltage drop range. And both APF and voltage compensator compensate asymmetries caused by nonlinear loads. Finally, two methods of detecting the negative sequence are reviewed, and the validity of this scheme is investigated through analysis of simulation and experimental results for a prototype active power filter system rated at 10KVA.

Key Words : APF, Voltage compensator, Unbalanced load, Negative sequence

1. Introduction

In typical distribution systems, the proliferation of non-linear loads, such as diode or thyristor rectifier, results in a deterioration of the quality of voltage waveforms at the point of common coupling (PCC) of various loads. To mitigate harmonic related problems, utilities increasingly enforce IEEE519, the recommended harmonic standard, particularly for large and industrial customers. It is important to note that IEEE519 harmonic standards are only applicable at the point of common coupling (PCC) of the utility-plant interface [1][2].

* Corresponding author
Tel. : +82-2-2290-0341
Fax. : +82-2-2297-1569
E-mail : woocheol@ihanyang.ac.kr

Conventional APFs can compensate the reactive and harmonic current of load. But due to the finite (nonzero) internal impedance of the utility source, which is simply represented by *Ls, Rs*, the voltage waveform at the PCC to other loads will become distorted and the voltage drop happens[3]. APF systems should operate and meet IEEE 519 harmonics standards under all supply and load conditions, such as, in the presence of maximum allowable 5% supply voltage harmonics, ± 10% supply voltage swells/sags, up to 10% supply voltage unbalance, and in the presence of supply current sub-harmonics. So, if PCC voltage drops up to 10%, APF cannot be adequately operated, and in this case voltage drop is more serious than harmonic current. The voltage drops are caused by flickers, direct-starting of motors, and in this case the proportion of the linear load is higher than that of the nonlinear load. So harmonic current is no longer a serious problem. Thus, we need to

switch the operation mode from APF to voltage compensator.

Unbalanced source currents cause asymmetric voltages in the network. The quality of the power supply is decreased[4]. But the parallel active filters permit to compensate the harmonics and asymmetries of the source current caused by nonlinear unbalanced loads[5]. Namely the first harmonic negative sequence component of the load currents can be determined and injected in opposite phase, thereby achieving the balancing function. The source current will constitute the first harmonic positive sequence system.

The APFs presented in this paper have some advantages: Firstly, when PCC voltage is within the 15% voltage drop range, reactive power and harmonics compensation are achieved. Secondly, when PCC voltage is not within the 15% voltage drop range, constant PCC voltage is achieved by switching from APF to voltage compensator. Thirdly, in order to improve the APF performance, a DC voltage control loop is implemented in both cases. Fourthly, both APF and voltage compensator have a function of compensating the negative sequence. Finally, two methods of detecting the negative sequence are reviewed, and validity of the proposed control algorithm is demonstrated in two ways: 1) Analysis of the results of computer simulation and 2) A prototype experiment.

2. Parallel Active Filter System

Fig. 1 shows the proposed system configuration of parallel APF with the e_a, e_b,, *and* e_c as AC source voltages, V_{pa} , V_{pb} , V_{pc} as PCC (Point of Common Coupling) voltage, and L_f and R_f forming a small passive filter to reduce the pulse width modulation (PWM) switching ripples generated from inverter of the APF.

2.1 Parallel Active Power Filter

The equivalent transfer function of the parallel APF, G, is shown in the following equation [6] ;

$$\mathbf{G(s) = kG_n e^{-\tau s} \frac{\omega_0}{S + \omega_0}}, \qquad (1)$$

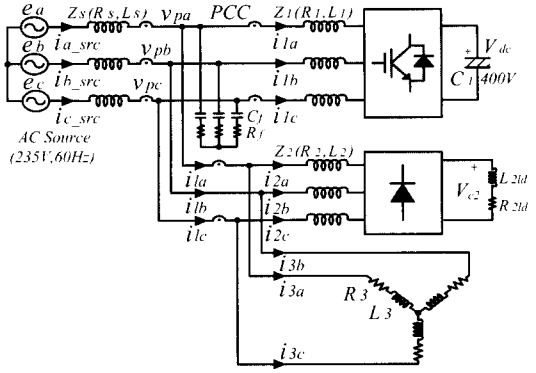

Fig. 1. System configuration of a parallel active filter.

In this equation, k is the equivalent gain ($k = 1 \pm 0.01 \sim 1 \pm 0.1$, the error results from the precision of current sensors and current control) and G_n is the equivalent transfer function of the harmonic detection circuit. The compensation characteristics can be obtained through the following equation.

$$\left|\frac{\mathbf{I_{src}}}{\mathbf{V_{c2}}}\right|_{e_s=0} = \left|\frac{1}{\mathbf{Z_s} + \mathbf{Z_2}/(1-\mathbf{G})}\right| \qquad (2)$$

Fig. 2 shows the calculated values. It is clear that, the smaller the load impedance (Z_2) is, the worse the compensation characteristics in parallel APF.

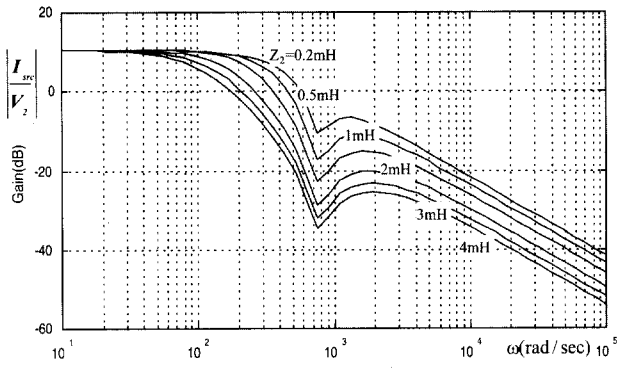

Fig. 2. Compensation characteristics of a parallel active filter for a harmonic voltage source with different impedance.

2.2 PCC Voltage Compensator

2.2.1 Voltage Regulation Without a PCC Voltage Compensator

Fig. 3 shows equivalent circuit of load and supply system [7]. Voltage E and V denote source voltage and PCC voltage respectively. In the absence of a voltage compensator, the PCC voltage drop caused by the load current, i_ℓ, is shown in Fig. 3(b) as $\Delta \mathbf{V}$

$$\Delta V = \Delta V_R + \Delta V_X \tag{3}$$

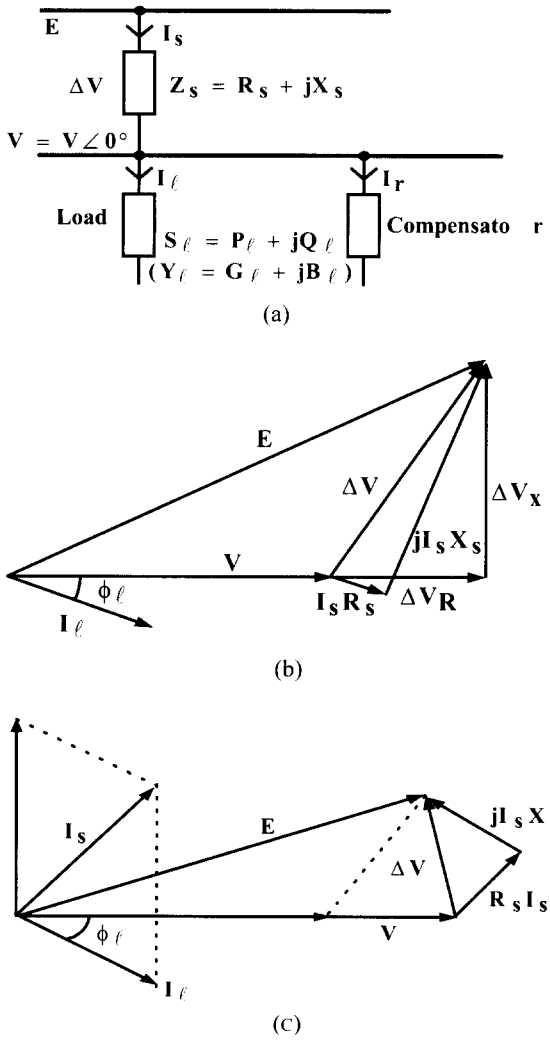

Fig. 3. Equivalent circuit and vector diagram : (a) Generated diagram for improvement of voltage regulation, (b) Vector diagram without voltage compensator, (c) Vector diagram with voltage compensator.

The voltage change has a component ΔV_R in phase with V and a component ΔV_X in quadrature with V, which are illustrated in Fig. 3(b). It is clear that both magnitude and the phase of V, relative to the supply voltage E, are functions of the magnitude and phase of the load current, namely, the voltage drop depends on both the real and reactive power of the load. The component ΔV is rewritten as

$$\Delta \mathbf{V} = \mathbf{I}_s\mathbf{R}_s + \mathbf{jI}_s\mathbf{X}_s \tag{4}$$

2.2.2 Voltage Regulation With a PCC Voltage Compensator

Fig. 3(c) shows vector diagram with voltage compensation. By adding a compensator in parallel with the load, it is possible to make $|\mathbf{E}| = |\mathbf{V}|$ by controlling the current of the compensator.

$$I_s = I_l + I_r \ (\mathbf{I}_r : \text{compensator current}) \tag{5}$$

However, phase differences between voltage E and V increase.

2.2.3 Comparison of APF with Reactive Power Compensation and a Voltage Compensator

APF can compensate the reactive power and the current harmonic components in nonlinear loads so that it can control the power factor. Reactive power compensation is achieved by sensing and computing the reactive component of the load current. Although reactive power is compensated by APF, PCC voltage drops because of line impedance. The voltage compensator can make $|\mathbf{E}| = |\mathbf{V}|$ by controlling the current of compensator, at the expense of phase between voltage E and V. By using the reactive current in APF, the voltage compensator compensates the PCC voltage drop caused by the reactive/active load current. And the voltage compensator needs the minimum active current to keep the DC link voltage constant. Therefore, the APF rating is determined by the reactive current of the voltage compensator.

Fig. 4 shows the two functions cannot be satisfied simultaneously. The vector diagram of APF with

reactive current compensation is explained by E', V, ΔV, I_s', and I_r'. By controlling the APF current, I_r', it can make the phase between I_s', and V the same.

But voltage drop would be happened, because of source impedance carrying the load current. The vector diagram for compensation of the PCC voltage is explained by E, V, ΔV, I_s, and I_r. By controlling the compensator current, I_r, the amplitude and phase of the source current, I_s, are changed to be $|\mathbf{E}| = |\mathbf{V}|$, but source current is leading.

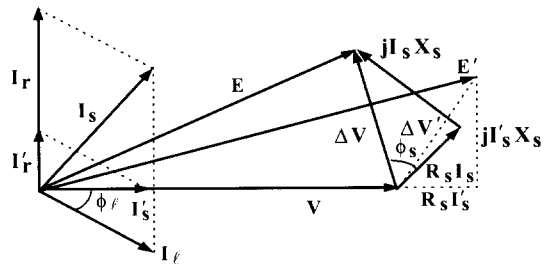

Fig. 4. vector diagram of compensation between APF and voltage compensation ($\mathbf{I}_r'$, $\mathbf{I}_s'$, $\mathbf{E}'$, $\mathbf{V}'$: APF with power factor correction, $\mathbf{I}_r$, $\mathbf{I}_s$, $\mathbf{E}$, $\mathbf{V}$: voltage compensator).

If the PCC voltage is within a certain range (15% voltage drop), the proposed APF operates as an APF. If the PCC voltage is out of that range, the APF performs as a voltage compensator. When a motor is started directly without special equipment, a large load current flows. So, PCC voltage will be out of range, and the nonlinear load and linear load mix together, and the portion of linear load becomes much bigger than the nonlinear load. Therefore, when voltage compensator is operated, we can observe the effect of decreasing the harmonics without harmonic compensation. After the motor starts and is going, the load current decreases, so PCC voltage is within a range (15% voltage drop). At that time, the proposed APF performs as an APF.

3. Parallel Active Power Filter Implementation

Fig. 5 shows synchronous reference frame controller for a proposed APF. It consists of current and voltage detector, DC bus voltage controller, PCC voltage controller, and current controller [8][9].

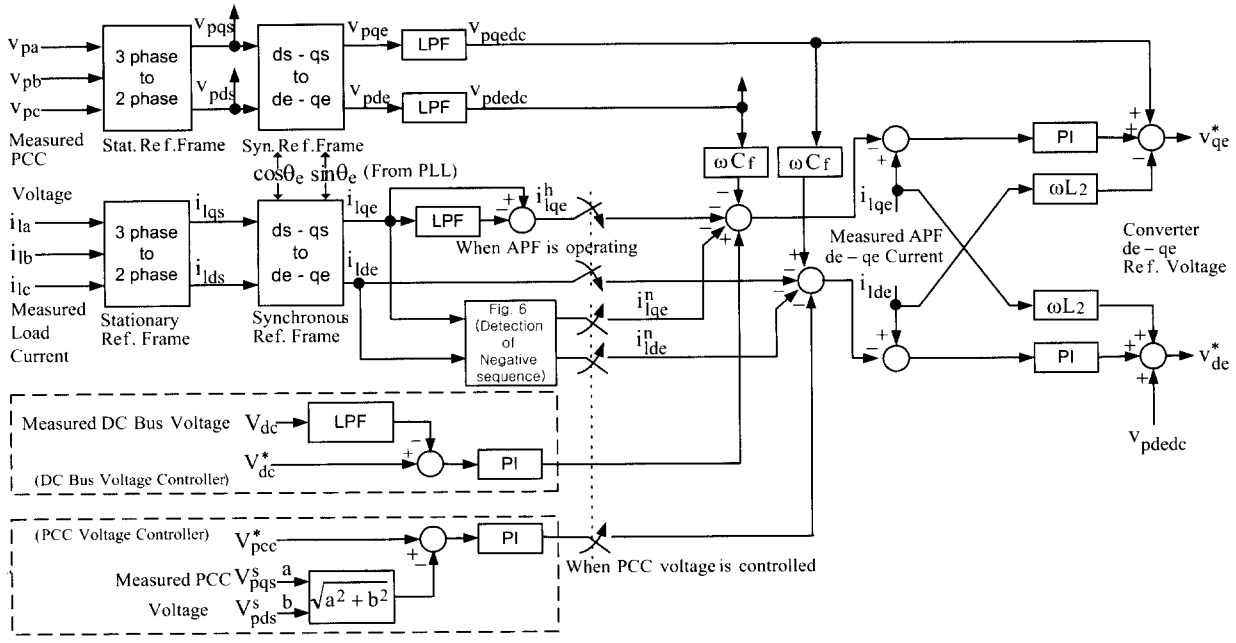

Fig. 5. Synchronous reference frame controller for a proposed APF.

3.1 The Detection of Load Current and PCC Voltage

The load current, i_l, is measured and extracted in the synchronous $d^e - q^e$ reference frame. Since these currents to be extracted are DC in both d^e and q^e axis. Filtering of the signal in the synchronous $d^e - q^e$ reference frame is insensitive to any phase errors introduced by low-pass filters. To extract the load current harmonics in synchronous $d^e - q^e$ reference frame, the high-pass filter implementation is realized as (1-LPF). The low pass filters used in this controller implementation are realized with cut-off frequency of 10Hz.

But in the synchronous d^e - q^e reference frame, current $i_{lds}{}^e$ is not filtered by LPF. That is because it needs to supply both reactive current and harmonics. When the proposed APF operates as an APF, negative sequence component of load current is harmonic. So negative sequence component is compensated without extra manipulation. The filter (including R_f and C_f) is needed to reduce the switching ripples generated by the inverter of the APF. So, to acquire the exact control, it should be compensated. But the impedance ratio of C_f is much higher than that of R_f, so only effects of C_f is considered.

3.2 DC Bus Voltage Control

The DC bus controller generates a fundamental reference to provide the real power transfer required to regulate the DC bus voltage and for compensation of the inverter losses.

The measured DC bus voltage V_{dc} used for feedback requires filtering to attenuate ac components present in V_{dc}. The dominant ac components of V_{dc} are at 360Hz and its multiples. In the presence of a supply voltage and load unbalance, the fundamental negative sequence component of the APF current will result in a 120 Hz V_{dc} ripple component. The 120Hz V_{dc} component needs to be detected and controlled, to minimize its adverse effect on APF current regulation. Hence, this 120Hz V_{dc} component is not filtered, and therefore the low-pass filter cut-off frequency is set at 150Hz.

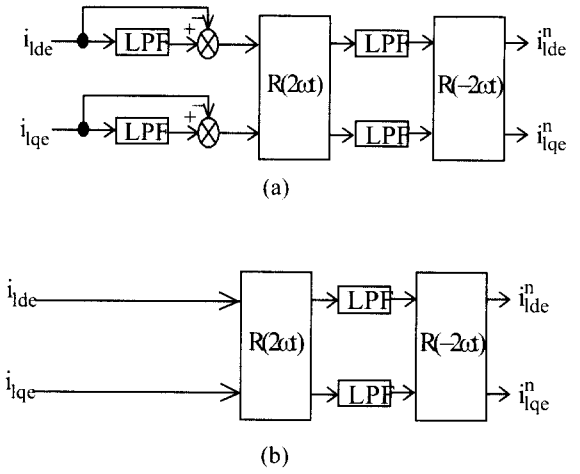

Fig. 6. The detection method of the negative sequence in load current : (a) The separation of negative sequence from load current filtered by LPF, (b) The separation of negative sequence from load current.

3.3 PCC Voltage Controller and detection of unbalanced load current

If PCC Voltage drops for some reason, such as the motor's direct starting, a proposed APF is needed to change the operation mode from APF to the PCC voltage compensation mode. However, when we change the operation mode, we also change the PI gain of the current controller. This causes a transient state, but due to the existence of reactors in source line, the real response is not much affected by the transient state. If we use the predictive or hysteresis current controller, then we do not have to be concerned with the PI gain.

Fig. 6(a) shows the detection method of the negative sequence in load current.

The unbalanced current can be divided into positive, negative and zero sequence components. But zero sequence is a null in Y-connection system. The positive sequence of load current is transformed into dc component and the negative sequence of load current is transformed into 120 Hz component in SRF (synchronous reference frame).

$$HPF\left(\begin{bmatrix} i_{lde} \\ i_{lqe} \end{bmatrix}\right) = R(-2\omega t)\begin{bmatrix} i^n_{lde} \\ i^n_{lqe} \end{bmatrix} + \begin{bmatrix} i^h_{lde} \\ i^h_{lqe} \end{bmatrix} \quad (6)$$

$$R(\omega t)=\begin{bmatrix} cos(\omega t) & -sin(\omega t) \\ sin(\omega t) & cos(\omega t) \end{bmatrix} \quad (7)$$

Equation (6) shows that the components through the HPF have negative sequence and harmonic component.

The negative sequence of the load current also becomes the reference of current controller when the proposed APF is operated as conventional APF, because the negative sequence is 120 Hz component in positive sequence SRF[10]. But when the proposed APF is operated as voltage compensator, it is needed to make the negative sequence be DC component by (8).

$$R(2\omega t)\cdot HPF\left(\begin{bmatrix} i_{lde} \\ i_{lqe} \end{bmatrix}\right)=\begin{bmatrix} i_{lde}^{n} \\ i_{lqe}^{n} \end{bmatrix}+\begin{bmatrix} i_{lde}^{h} \\ i_{lqe}^{h} \end{bmatrix}R(-2\omega t) \quad (8)$$

The only negative sequence component can be extracted by using the LPF. The separated i_{de}^{n}, i_{qe}^{n} have much less ripples because there is no positive sequence to be removed.

Fig. 6(b) shows another detection method of the negative sequence in load current. Negative sequence of load current is transformed into DC component through the LPF in negative SRF, but positive sequence of load current is comparatively larger than negative sequence. Therefore, if it is through low order LPF, not only DC component but 120Hz ripple component of positive sequence is left a lot. Hence, high order LPF is necessary for removing the positive component. Eq. 9 is for making the negative sequence be DC component.

$$R(2\omega t)\cdot HPF\left(\begin{bmatrix} i_{lde} \\ i_{lqe} \end{bmatrix}\right)=\begin{bmatrix} i_{lde}^{n} \\ i_{lqe}^{n} \end{bmatrix}+\begin{bmatrix} i_{lde}^{p} \\ i_{lqe}^{p} \end{bmatrix}R(2\omega t)+\begin{bmatrix} i_{lde}^{h} \\ i_{lqe}^{h} \end{bmatrix}R(-2\omega t) \quad (9)$$

4. Experimental Results

In order to implement the proposed APF, a single 32-bit floating-point DSP, TMS320C31, with the single-cycle execution time of 60*n*sec and a 10kVA laboratory prototype using IGBT switches was used. The switching period for the PWM was 150 μsec.

Table 1 System Parameters.

Parameters	Value
Input voltage(e_a, e_b, e_c)	235V, 60Hz
Line impedance (Rs , Ls)	0.3 Ω , 1mH
Input filter (Rf , Cf)	2 Ω , 50 μF
Input impedance (L1)	1.3mH
Input impedance (L2)	0 mH
DC link capacitor (C1)	14,800 μF
Load I (R_{2ld}, L_{2ld})	16 Ω , 0.15 mH
Load II (R3 , L3)	3 Ω , 9mH
Load II (R3 , L3): Unbalance(R,S,T)	R(3 Ω ,7mH),S(3 Ω ,7mH), T (8 Ω ,11mH)
DC link voltage (Vdc)	400 Vdc

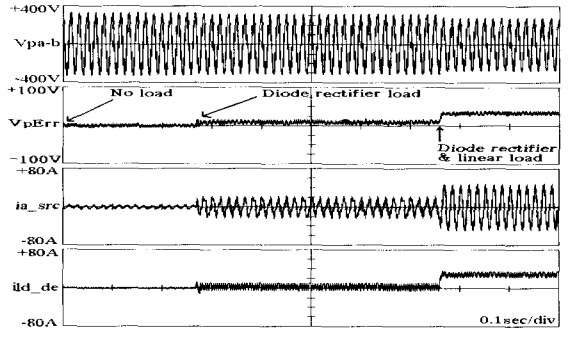

Fig. 7. PCC voltage variation when load is changing from diode rectifier to diode rectifier and linear load without active power filter ($V_{pa\text{-}b}$: line to line voltage of PCC , V_pErr : error of PCC voltage, i_{a_src}: source current of phase a, i_{ld_qe}: q-axis load current in synchronous ref. frame).

Table 1 shows system parameters, load condition under the unbalance.

Input impedance (R_s, L_s) consisted of somewhat large values having a 50:50 impedance ratio. The somewhat large values were chosen because of the limitations of the small capacity of inverter used in the experiment.

Fig. 7 shows the PCC line-to-line voltage drop according to load variation without any compensation. Although no load was connected, there was a source current (i_{a_src}) because of filter current (L_f,C_f). When the diode rectifier load was applied, the PCC voltage dropped a little. But when a linear load was applied additionally, the PCC voltage dropped seriously ($235V_{rms} \rightarrow 195V_{rms}$, 17% voltage drop).

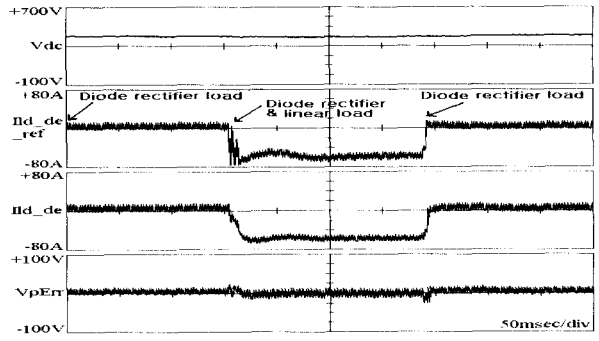

Fig. 8. active filter response when load is changing from diode rectifier load to diode and linear load (V_{dc} : DC voltage in active filter, $i_{ld\_de\_ref}$: reference of reactive current, i_{ld_de} : reactive current of load, V_pErr : error of PCC voltage).

Fig. 8 and 9 show APF responses when load is changing from diode rectifier to diode rectifier and linear load. As a diode rectifier load, and in order to make the harmonic current sources, instead of using the capacitor, reactor (C_2, L_2), the resistor and inductor (R_{2ld}, L_{2ld}) were used in a DC link.

As a linear load, the resistor and inductor (R_3, L_3) were used with Y connection. This is the equivalent model of the motor having a power factor 0.6. As an unbalanced R-L load, unbalanced impedance ratio of the resistor and inductor (R_3, L_3) was about 45%.

Fig. 8 shows that output reactive current follows the reference reactive current properly, when the diode rectifier load was applied to the PCC, there was some error of PCC voltage, so the proposed APF operated as an APF. When the linear load was applied additionally, there was little error of PCC voltage. That's because the proposed APF operated as a voltage compensator. Especially, when it was operated as a voltage compensator, the PCC voltage was compensated by 97% of nominal voltage($235V_{rms} \rightarrow 229V_{rms}$, 2.5% voltage drop).

Fig. 9(a) shows APF response when load is changing from diode rectifier to diode and linear load.

When the diode rectifier load was applied to the PCC, the proposed APF operated as an APF. This was because there was only minimal PCC voltage drop and the source current was controlled as having a high power factor and lower harmonics.

When linear load was applied additionally, voltage drop of PCC was serious, so the proposed APF operated as a voltage compensator. Therefore, the PCC voltage was controlled constantly as shown in Fig. 8. But the source current was leading. Fig. 9(b) shows the same waveforms in Fig. 9(a). But the time scale is enlarged from 40*msec/div* to 20*msec/div*.

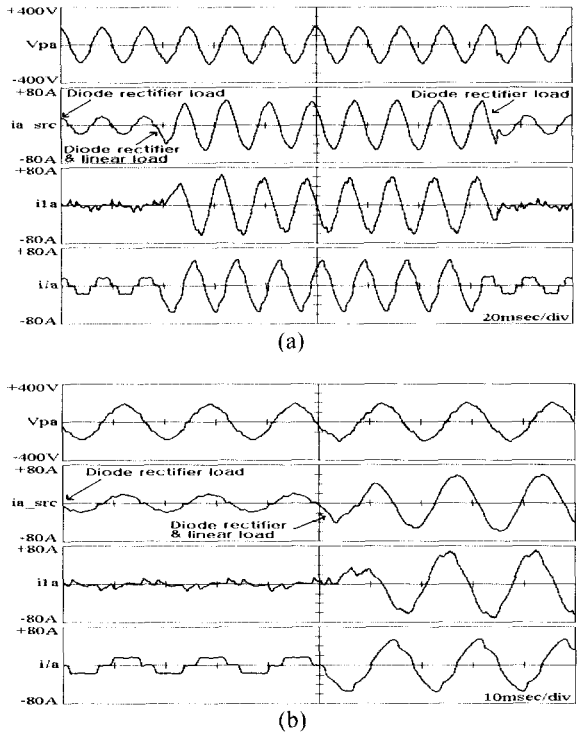

Fig. 9. APF response when load is changing from diode rectifier to diode and linear load (V_{pa} : PCC voltage of phase *a*, i_{a_src} : source current of phase *a*, i_{fa} : APF current of phase *a*, i_{la} : load current of phase *a*) : (a) When time scale is 20*msec/div*, (b) When time scale is 10*msec/div*.

Fig. 10(a) shows the THD of source current when the proposed APF was operated as an APF and only diode rectifier load was applied. The THD of source current was about 6.94%. Fig. 10(b) shows the THD of source current when the proposed APF was operated as a voltage compensator, and both diode rectifier and linear load were applied. The THD of source current was about 4.74%. Fig. 10(b) was less distorted than Fig. 10(a) that is because the proportion of linear load was much higher than that of nonlinear load.

Fig. 11 shows unbalanced load currents, they consisted of unbalanced R-L load, which has unbalanced impedance ratio of 45%, and balanced diode load.

Fig. 12 to Fig. 15 show the proposed APF when it was operated under the unbalanced load. Fig. 12 shows when it was operated as an APF without the compensation of negative sequence current. It shows source currents were much unbalanced.

Fig. 13 shows when it was operated as an APF with the compensation of negative sequence current. It shows source currents were slightly unbalanced. But both waveforms of source currents were almost the same.

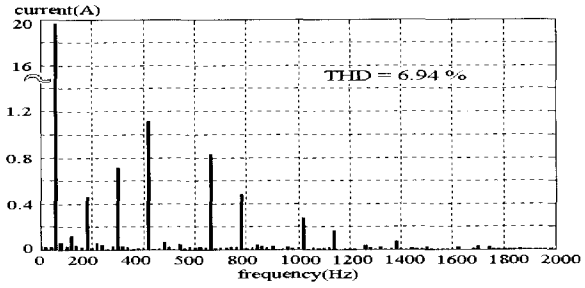

Fig. 10. The THD of source current : (a) In case of an APF, (b) In case of voltage compensator.

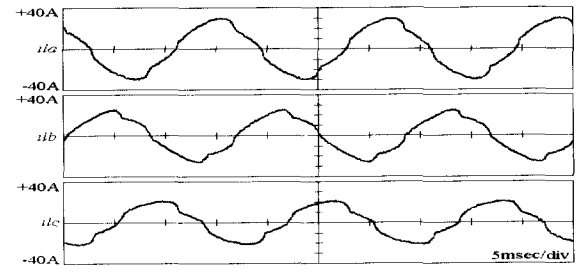

Fig. 11. Unbalanced three-phase load current (*ila*, *ilb*,*ilc* : load current of phase *a*, b, c).

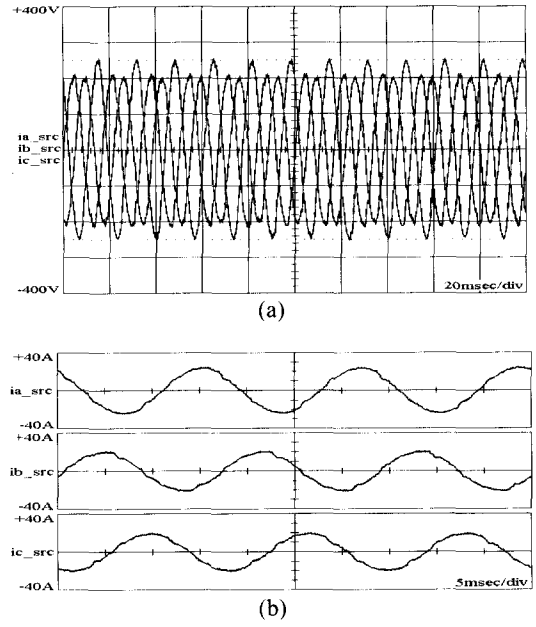

Fig. 12. Source currents when proposed APF is operated as APF without the compensation of negative sequence current under unbalanced load (*ia_src* : source current of phase *a*,, *ib_src* : source current of phase b, *ic_src* : source current of phase c) : (a) When time scale is 20msec/div, (b) When time scale is 5msec/div.

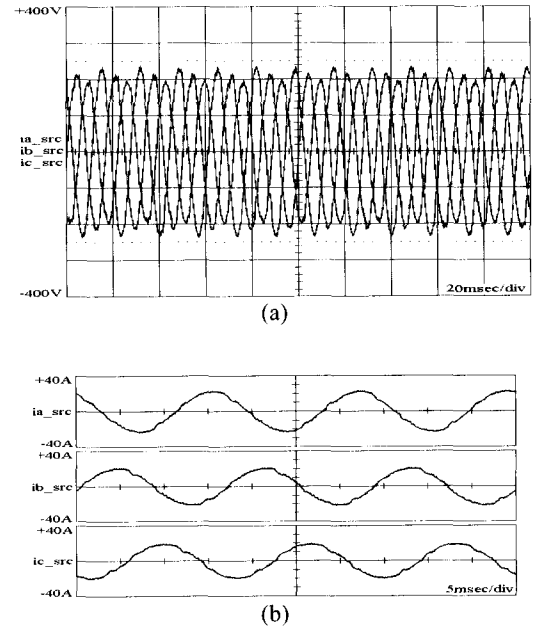

Fig. 13. Source currents when proposed APF is operated as APF with the compensation of negative sequence current under unbalanced load : (a) When time scale is 20msec/div, (b) When time scale is 5msec/div.

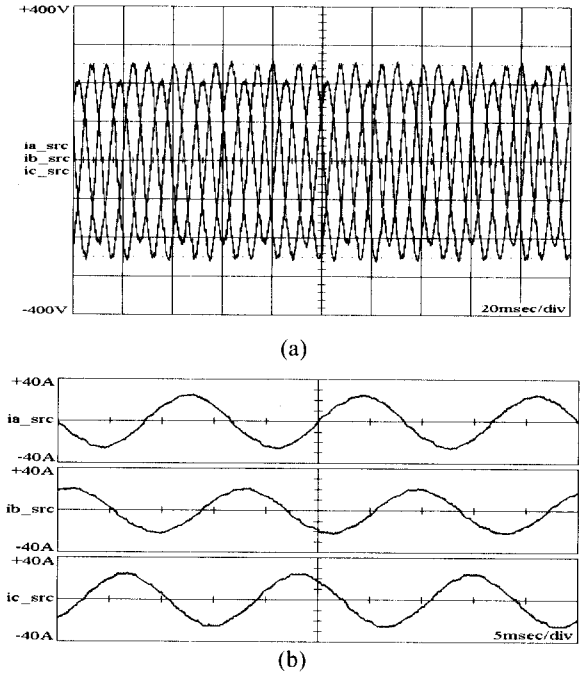

Fig. 14. Source currents when proposed APF is operated as voltage compensator without the compensation of negative sequence current under unbalanced load : (a) When time scale is 20msec/div, (b) When time scale is 5msec/div.

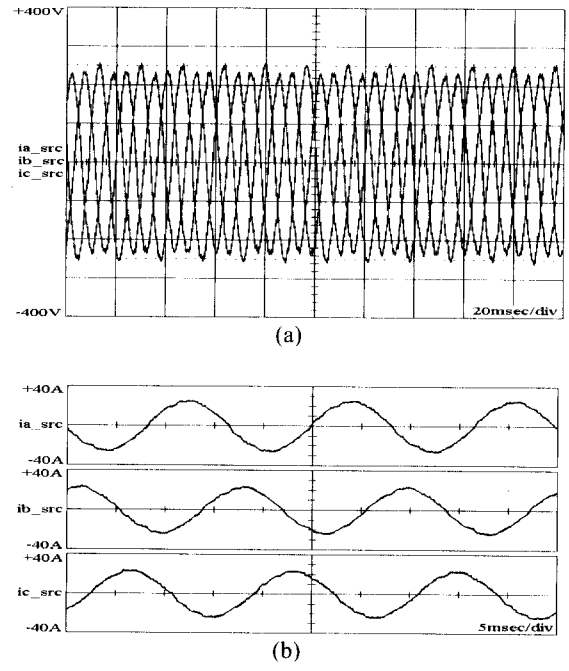

Fig. 15. Source currents when proposed APF is operated as voltage compensator with negative sequence current compensation under unbalanced load : (a) When time scale is 20msec/div, (b) When time scale is 5msec/div.

Fig. 14 shows when it was operated as a voltage compensator without the compensation of negative sequence current. It shows source currents were much unbalanced.

Fig. 15 shows when it was operated as a voltage compensator with the compensation of negative sequence current. It shows source currents were a little unbalanced. But both waveforms of source currents were almost same.

5. Conclusion

This paper proposed a three-phase parallel active power filter operation with PCC voltage compensation considering the unbalanced load, and compared functions of APF and voltage compensator. The proposed scheme has two operation modes. Firstly, it operates as an active power filter with reactive power compensation when PCC voltage is in a certain range (15% voltage drop). Secondly, when the PCC voltage is out of certain range (15% voltage drop), it operates as a voltage compensator. And both APF and voltage compensator compensate asymmetries caused by nonlinear loads. And two methods of detecting the negative sequence are reviewed. To test the validity of the proposed scheme, simulation and experimental results were analyzed. Although promising results were obtained, further research needs to be done related to current controllers and negative sequence.

References

[1] S. Bhattacharya and D. M. Divan, "Synchronous frame based controller implementation for a hybrid series active filter system," *IEEE/IAS Annu. Meeting*, 1995, pp. 2531~2540.

[2] L. A. Mohan, J. W. Dixon, R. R. Wallace, "A three-phase active power filter operating with fixed switching frequency for reactive power and current harmonic compensation," *IEEE Trans. On Ind. Elec.*, vol. 42, no. 4, pp. 402~408, August 1995.

[3] H.Akagi, "Trends in active power line conditioners," *IEEE Trans. On Power Electronics*, vol. 9, no. 3, pp. 263~268, May 1994.

[4] P.Verdelho and G.Marques, "An Active Power Filter and

Unbalanced Current Compensator," *IEEE Trans. On Industrial Electronics*, vol. 44, pp. 321~328, June 1997.

[5] F.-Z. Peng, H.Akagi, and A. Nabae, "A study of active power filters using quad-series voltage-source PWM converters for harmonic compensation," *IEEE Trans. Power Electron.*, vol. 5, pp. 9~15, 1990.

[6] F. Z. Peng, "Application issues of active power filters," *IEEE Industry Applications Magazine*, vol. 4, no. 5, pp. 21~30, Sep./Oct. 1998.

[7] T. J. E. Miller, *Reactive Power Control in Electric Systems*, John Wiley &Sons, a Wiley-Interscience Publication, 1982.

[8] S. Bhattacharya, T. M. Frank, D.M. Divan, and B.Banerjee, "Parallel active filter implementation and design Issues for utility interface of adjustable speed drive systems," *IEEE/IAS Annu. Meeting*, 1996, pp. 1032~1038.

[9] Schauder, CD., and Mehta, H., "Vector analysis and control of advanced static var compensators," *IEE Fifth International Conference on AC and DC Transmission*, London, Conference Publication No. 345, pp. 266~272, 1991.

[10] P. Verdelho, "An Antive Power Filter and Unbalanced Current Compensator," *IEEE Trans. Ind. Electron.*, vol. 44, no. 3, pp. 321~328, 1997.

Woo-Cheol Lee was born in Seoul, Korea in 1964. He received the B.S. and M.S. degrees in electrical engineering from Hanyang University, Seoul, Korea, in 1987 and 1989, respectively, where he is currently pursuing the Ph.D degree in electrical engineering. From 1988 to 1998, he was with the R&D Institute, Hyosung Industries Company Ltd., as a Senior Researcher, Seoul, Korea.

Taeck-Kie Lee was born in Seoul, Korea, in 1963. He received the B.S., M.S. and Ph.D. degrees in electrical engineering from Hanyang University, Seoul, Korea, in 1987, 1989 and 1993, respectively. From 1994 to 1996, he was with the Department of Electrical Engineering, Seonam University, Namwon, Korea. Since 1996, he has been with Hankyong National University, Ansung, Korea, where he is an Associate Professor with the Department of Electrical Engineering.

Dong-Seok Hyun received the B.S. and M.S. degrees in electrical engineering from Hanyang University, Seoul, Korea, in 1973 and 1978, respectively, and the Ph.D. degree in electrical engineering from Seoul National University, Seoul, Korea, in 1986. He was a Research Associate in the department of Electrical Engineering, University of Toledo, Toledo, OH, from 1984 to 1985 and a Visiting Professor in the department of Electrical Engineering at the Technical University of Munich, Germany, from 1988 to 1989. Since 1979, he has been with Hanyang University, where he is currently a Professor in the department of Electrical Engineering.